Arctigenin Exerts Neuroprotective Effect By Ameliorating Cortical Activities in Experimental Autoimmune Encephalomyelitis in Vivo

Liangpeng Wei
Tianjin Medical University https://orcid.org/0000-0002-7921-4532
Zhenyi Xue
Tianjin Medical University
Baihui Lan
Tianjin Medical University
Shiyang Yuan
Tianjin Medical University
Yuanyuan Li
Shandong University of Traditional Chinese Medicine
Cunle Guo
Tianjin Medical University
Rongxin Zhang
Guangdong Pharmaceutical University
Ran Ding
Peking University Academy for Advanced Interdisciplinary Studies
Hui Shen (shenhui@tmu.edu.cn)
Tianjin Medical University https://orcid.org/0000-0002-8195-8143

Research article

Keywords: EAE, Arctigenin, two-photon Ca2+ imaging, in vivo, cortical activity, AMPA receptor

Posted Date: January 25th, 2021

DOI: https://doi.org/10.21203/rs.3.rs-152500/v1

Abstract

Background

Multiple sclerosis (MS) is a chronic disease in the central nervous system (CNS), characterized by inflammatory cells invade into the brain and the spinal cord. Among a bulk of different MS models, the rodent model of experimental autoimmune encephalomyelitis (EAE) is the most widely used and best understood. Arctigenin, a botanical extract from Arctium lappa, is reported to exhibit pharmacological properties including anti-inflammation and neuroprotection. However, the effects of Arctigenin on neural activity attacked by inflammation in MS are still unclear.

Methods

Female C57BL/6 mice were expressed by an ultra-sensitive protein calcium sensor GCamp6f in somatosensory cortex neurons through stereotaxic virus injection. Then we induced EAE model in mice with myelin oligodendrocyte glycoprotein (MOG) peptide (35-55) and used two-photon calcium imaging to chronically observe cortical activity *in vivo* throughout the disease progression. Besides, we performed whole-cell electrophysiological recording to determine the frequency of α-amino-3-hydroxy-5-methyl-4-isoxazolepropionic acid (AMPA) receptor-mediated spontaneous excitatory postsynaptic current (sEPSC) in cortical brain slices of preclinical EAE mice.

Results

Here we found added hyperactive cells, calcium influx, network connectivity and synchronization, mainly at preclinical stage of EAE model. Besides, more silent cells and decreased calcium influx and reduced network synchronization accompanied by a compensatory rise in functional connectivity were found at the remission stage. Arctigenin treatment not only restricted inordinate individually neural spiking, calcium influx and network activity at preclinical stage, but also restored neuronal activity and communication at remission stage. In addition, we confirmed that the frequency of AMPA receptor-sEPSC was also increased at preclinical stage and can be blunted by Arctigenin.

Conclusions

Our findings suggest that excitotoxicity resulted from calcium influx is involved in EAE at preclinical stage. Moreover, Arctigenin exerts neuroprotective effect by limiting hyperactivity at preclinical stage and ameliorates EAE symptoms, indicating Arctigenin could be a potential therapeutic drug for neuroprotection in MS-related neuropsychological disorders.

Background

Multiple sclerosis (MS) is a chronic disease in which inflammatory processes attack the central nervous system (CNS) characterized by widespread inflammation, demyelination, gliosis, and neuropsychological disorders, resulting a huge healthcare burden [1, 2]. In classical theory, MS has been long hallmarked by

demyelinating lesions in the focal white matter [3]. However, with more investigation of MS, it is clear that detectable pathological changes have occur in normally appearing white matter, as well as in the CNS grey matter because of the presence of focal grey matter lesions and grey matter atrophy [4]. The analysis of functional connectivity obtained through resting-state functional magnetic resonance imaging (RS-fMRI), suggests a complex pattern of abnormal connection between the somatosensory network regions [5, 6]. Recent reports have demonstrated that patients and animals with MS suffer from cognitive impairment and neuropsychological dysfunction in preclinical stage [7-9], indicating the effects of inflammation on neuronal and synaptic in the earliest phases of MS [10].

As the most widely used model in MS research, experimental autoimmune encephalomyelitis (EAE) is usually accompanied by perivascular infiltration of leukocytes, demyelination and axonal damage in cerebral cortex and white matter [11]. Relapsing-remitting EAE (RR EAE) mouse models are suitable to imitate related aspects of relapsing-remitting MS (RRMS) [12]. In addition, it is reported that EAE leads cortical layer 5 neuron loss and atrophy of the whole cerebral cortex, which strongly correlates with axonal damage [13-15].

Arctigenin isolated from a herbal medicine, Arctium, lappa, acts as potent bioactive component, which was widely used in asian countries, especially in Korea [16, 17]. Arctigenin has been reported to exhibit several pharmacological properties, including antidepressant [18, 19], anti-*T. gondii* [20], anti-inflammatory [21] and neuroprotective effects [22]. Arctigenin can protect brain from ischemic stroke through inhibiting NLRP3 inflammasome activation [23]. Additionally, Arctigenin administration can protect dopaminergic neurons by eliciting potent antioxidant and anti-inflammatory effects and improve behavior changes of parkinson's disease [24]. Arctigenin treatment reduced hematoma, gene expressions of inflammatory (IL-6 and TNF-α) and apoptosis (Caspase-3 and Bcl-2), and accelerated wound closure after a stab wound injury, indicating Arctigenin possesses neuroprotective effects on brain tissue through anti-inflammatory and anti-apoptotic actions.

Recently, we have reported that Arctigenin can suppress the differentiation and proliferation of Th17 cells and ameliorate mice EAE symptoms [25]. However, the effects of Arctigenin on the central nervous system (CNS) in EAE animals *in vivo* are still unclear. Here, we used two-photon Ca^{2+} imaging to observe cortical activity in the somatosensory layer 2/3 cortex in living awake mice of EAE, and detected hyperactivity phenomenon exclusively at preclinical stage, including more hyperactive neurons, excessive calcium influx into cells, circuit functional connectivity and synchronization. Besides, we employed whole-cell patch-clamp recordings in acute brain cortex slices to record AMPA receptor mediated sEPSC in preclinic phase, the increased frequency of sEPSC was consistent with hyperactivity *in vivo*. Furthermore, increased fraction of silent neurons, reduced calcium influx and network synchronization were found at the remission stage, indicating impaired neuronal activity at the third stage of disease. Meanwhile, cortical functional connectivity stayed at a high level as a compensation. Administration of Arctigenin dramatically limited preclinically cortical hyperactivity and reversed the frequency of AMPAR-sEPSC to control level. Moreover, at remission stage, Arctigenin decreased the number of silent neurons, restored neuronal activity and synchronization, and inhibited maladaptive functional connectivity. These results

suggest that Arctigenin exerts neuronal protection effects in EAE through attenuating glutamate-induced neurotoxicity at early time.

Methods

Animals

We purchased 8-10-week-old female C57BL/6 mice from the institute of zoology, Chinese academy of sciences. All animals used were maintained under a 12 hr light/dark cycle and given enough food and water throughout the exprement and were housed in cages in the Tianjin medical university of China-approved animal facility. All experiments were supported by the Animal Care and Use Committee of Tianjin medical university, in accordance with National Institutes of Health guidelines.

Stereotaxic virus injection

Mice were anesthetized with isoflurane (1–1.5%) and intraperitoneally injected with analgesic buprenorphine (0.3 mg/kg). The glass pipettes used to perform virus injection were beveled at 45° with a 10–15 μm opening. We inserted a suitable micro sample syringe controlled by a hydraulic manipulator (Narashige, MO10) into the pipette and backfilled the system with mineral oil when we loaded or infused the viral solution. To avoid virus leakage before arriving the injection site, we filled the tip of glass pipette with ~1nl saline before virus injection. After infusing solution, we kept the pipette in the brain for about ten minutes and then withdrawn the syringe (~1 nl in volume) before pulling up the pipette to avoid backflow during withdrawal. About 30nl volume of rAAV-hsyn-GCaMp6f-WPRE-hGH-containing solution (~ 2×10^{13} infectious units / ml) was injected into somatosensory cortex slowly (AP: ~ -1.5mm, ML: ~ 2.0mm) for imaging calcium activity with GCaMP6f.

Craniotomy surgery

Two weeks after virus injection, mice were anesthetized with isoflurane (1–1.5%) and injected with the analgesic buprenorphine (0.3 mg/kg). The skin on top of head was removed after local lidocaine injection (2%), and we performed a round craniotomy (~4mm diameter) over the somatosensory cortex carefully and intermittently, using a cranial drill possessing a precisely machined tip steel burr with 0.5 mm in diameter. For better imaging results, the dura mater was removed by a forceps with care taken to avoid damage to the cortex surface and blood vessels. A round glass coverslip (5mm in diameter) was sticked over the opening with biological glue. We used dental cement and cyanoacrylic glue (UHU) to fix the custom-made chamber onto the skull. After dental cement set, mice were put back to cage and intraperitoneally injected with cephalosporin for 3~5 days to prevent infection at the craniotomy window. After craniotomy surgery, mice were allowed to recovery for one week.

Induction and treatment of EAE

To induce EAE, we injected mice (C57BL/6aged 8-10 weeks) with myelin oligodendrocyte glycoprotein (MOG residues35–55). The sequence of peptide was Met-Glu-Val-Gly-Trp-Tyr-Arg-Ser-Pro-Phe-Ser-Arg-Val-Val-His-Leu-Tyr-Arg-Asn-Gly-Lys, and the peptide purity was more than 95 % (CL. Bio-Scientific Co., LTD., Xi'an, China). We admixed 100μg MOG35–55 peptide and complete Freund's adjuvant containing 5mg/ml of heat-killed H37Ra, a *Mycobacterium tuberculosis* strain (Difco Laboratories). And then the mixture was injected into mice subcutaneously. Pertussis toxin (400ng) (List Biological Laboratories) in PBS and NaCl (50mM) was administered i.p. subsequently and the second time after 24 h [25]. Due to the stability of EAE induction with MOG residues35–55, 8 mice we induced for calcium imaging all showed clinical symptoms. Mice were randomly divided into two groups, one group was treated with Arctigenin. For the intervention of EAE, Arctigenin was injected (10 mg/kg, i.p.) daily from the first day after EAE induction, and DMSO was administrated as control. We purchased Arctigenin (purity > 98%) from Tianjin Shilan Technology company. To assess the disease symptoms, we used the below standard rating scale: 0, no obvious changes in motor functions; 1.0, limp tail; 2.0, limp tail and wobbly gait; 3.0, bilateral hind limb paralysis; 4.0, complete hindlimb and partial forelimb paralysis; and 5.0, death.

Two-Photon Ca^{2+} Imaging *in vivo*

A commercial Nikon A1R two-photon microscope system was used to perform two-photon calcium imaging. Two-photon excitation beam was emitted by a mode-locked Ti: Sa laser (model "Mai-Tai Deep See", Spectra Physics). We utilized a water-immersion objective (Nikon) with 25 × /1.10NA to perform imaging. The excitation wavelength was set to 910nm for Gcamp6f calcium imaging experiments. For somatic imaging, the dimension of field-of-view (FOV) was set 200μm × 200μm. We acquired images of 512 × 512 pixels at 30Hz frame rate. The average power reaching the cortical surface ranged from 30 to 40mW, depending on the expression efficiency of virus and depth of imaging. Within an imaging time window of ~3 min (~1min per time, 3 times in total) for each imaging, no sign of photo-damage was observed. Before the experiment, the mice were fixed under microscope objective frequently with the chamber to adapt to the imaging state for real calcium activity.

Electrophysiological recording

Separate 7 mice underwent EAE induction for electrophysiological recording. We randomly chose 3 mice to inject Arctigenin (10 mg/kg, i.p.) daily after induction. Day7 to day9 after induction, Mice under deeply anesthetization by breathed in isoflurane were decapitated. The brains were rapidly dissected in precooled, oxygenated standard artificial cerebrospinal fluid (ACSF) (120mM NaCl, 2.5mM KCl, 2.4, 1.25mM NaH_2PO_4, 26mM $NaHCO_3$, 2mM $MgSO_4$, 2mM $CaCl_2$, 10mM d-glucose; pH: 7.4). Both hemispheres were sliced coronally (350um) in cold ACSF. The slices containing somatosensory cortex were quickly transferred to 32℃ ACSF for 30 minutes and then incubated at room temperature for at least 1 h. The slice was fixed in a recording chamber that was set on the fixed-stage of an upright Olympus BX50WI microscope (Olympus). The oxygenated ACSF was perfused through recording chamber continuously. Pyramidal neurons in layer 2/3 were optically identified and whole-cell patched for recording. Picrotoxin (50 μM), D-AP5 (20 μM), and TTX (1μM) were applied to pharmacologically isolate

the AMPA receptor-mediated sEPSCs, with voltage clamp-mode at −70 mV. The resistance of glass pipettes for recording were 5–7 MΩ (intracellular solution containing: 130mM $CsMeSO_3$, 8mM NaCl, 10mM HEPES, 0.3mM Na-GTP, 4mM Mg-ATP, 5mM QX314, 0.2mM EGTA; pH: 7.3). An Axon 700B amplifier (AXON Instrument) was utilized to record the electrical signals. The data were digitized at 20 kHz and filtered at 10 kHz by using a Digidata-1440B system with pclamp 10.1 software (Molecular Device).

Data analysis

The calcium imaging data were calibrated for motion artifacts and analyzed with custom-written software in Matlab 8 (Mathworks). We visually identified and drawn regions of interests (ROIs) based on fluorescence intensity to acquire fluorescence signals from imaging data. The Ca^{2+} signals were represented by relative fluorescence changes calculated as $\Delta f/f = (f-f0)/f0$. In which f was estimated by averaging fluorescence of all pixels within each specified ROI, and f0 represented the baseline fluorescence of ROI estimated as the 25th percentile of the fluorescence within a sliding time window. Cortical functional connectivity is defined as a strong temporal correspondence of events between two neurons [26]. Drastic motion imaging data were excluded from the analyses. The Kolmogorov–Smirnov (K-S) test was used to determine normality of all data sets. Statistical significance was evaluated using Two-sample Mann-Whitney test or ANOVA with Kruskal-Wallis test. Distribution histogram and cumulative distribution were used to compare distribution difference of groups in different periods of EAE. Further experimental results were represented as mean ± SEM, $P < 0.05$ was regarded as statistically significant.

Results

Two-photon Ca^{2+} imaging in layer 2/3 of somatosensory cortex in vivo in living awake mice

We first injected an ultra-sensitive genetically encoded calcium indicator, GCaMP6f [27], into the layer 2/3 of somatosensory cortex (Fig. 1a, b). A chronic cranial window on cortex was established to observe neuronal activity in the awake mouse *in vivo* at least one month (Fig. 1d-f). Healthily control wild-type C57BL/6 mice exhibited spontaneous neuronal activity at different cortical depths (Fig. 1g). We induced EAE with myelin oligodendrocyte glycoprotein (MOG residues 35–55) injected into the mice via subcutaneous injection [25]. The values of the disease clinical score were recorded every day after EAE induction. According to the clinical scores, we classified the process of the disease to three stages: ‘preclinic’, ‘relapse’, and ‘remission’ stage (Fig. 1a, c). In the preclinic stage, there is no clinical symptom in EAE mice, while in the relapse and remission stage, the obvious symptom came up and lasted several weeks, and the healthy wild-type mice did not exhibit any clear clinical symptoms.

Arctigenin relieves EAE symptoms

Arctigenin was injected intraperitoneally every day (10 mg/kg) from the beginning after EAE induction to determine its effects on EAE. The Arctigenin-treated mice had a delayed onset of clinical symptoms,

approximately five days (Fig. 2a) compared with the vehicle-treated control mice. Besides, the Arctigenin-treated group had evidently reduced clinical scores throughout the disease. The severity of disease was assessed by cumulative and maximum clinical scores (Fig. 2b, c). EAE mice without Arctigenin treatment had significantly higher cumulative clinical score (40.55 ± 6.42) than Arctigenin-treated mice (22.00 ± 4.07) (Fig. 2b). These results suggest that Arctigenin extenuates the inflammatory impairment and relieves EAE mice's clinical symptoms.

Emergence of more hyperactive neurons in early EAE

To chronically monitor neurons activity in layer 2/3 of somatosensory cortex, we performed two-photon calcium imaging at 8:00 a.m. daily for about 40 days. Representative calcium images of the same region and activity traces of neurons at four time points in different periods of the experiment are showed (Fig. 3a, b). In healthily control mice, around 12% of neural population exhibited hyperactivity (>6 transients / min) throughout entire chronic recordings. Moreover, in EAE mice, the fraction of hyperactive cells also stayed at the same level with control group both in the relapse (13%) and remission stage (14%). However, it is noteworthy that, on the 7th day post EAE induction, we observed a significant increase (up to 40%) in the mean fraction of hyperactive neurons (Fig. 3c). This extraordinary proportion of hyperactive neurons indicates the change of cortical activity pattern in early EAE.

Arctigenin restricts the increase in fraction of hyperactive at preclinical stage and reduced silent neurons at remission stage of EAE *in vivo*

Based on the calcium transients, cells were further classified to three categories, inactive cell (no Ca^{2+} transient in recording time), normal cell (1- 6 Ca^{2+} transients/min), and hyperactive cell (> 6 Ca^{2+} transients/min) to observe the details of cortical activity in EAE (Fig. 4a, b). The distribution of hyperactive cell in activity map shows more hyperactive neurons in vehicle treated EAE mice on the 7th day after induction, while the increase was not obvious in Arctigenin treated mice (Fig. 4a). In addition, from the chronic recording of three kinds of cells, we found that the fraction of hyperactive cells abruptly increased as early as three days after EAE induction and remained high level for about a week. However, Arctigenin treatment made this increase slow and mild (Fig. 4e). Furthermore, the more inactive cells and less normally active cells appeared during late period in vehicle treated EAE mice while Arctigenin reversed these change (Fig. 4c, d). Apart from that, we summarized the fraction of three category cells in the preclinical stage (day 1 to day 10 after induction) and remission stage (day 19 to day 30 after induction) (Figure 4f, g). Notably, the percentage of hyperactive cells as well as normal cells in vehicle-treated EAE group was significantly increased compared to control mice at preclinical stage and Arctigenin reversed the increase to a considerable degree (Fig 4f). Meanwhile, at the remission stage of EAE, the fraction of inactive cells was obviously increased in vehicle treated mice and the normally active cells were reduced significantly, which means cortical silence during late period of disease. However, Arctigenin compromised these effects of EAE induction (Fig 4g). Taken together, these results demonstrate that Arctigenin limited the growing in numbers of cortical hyperactive neurons at preclinic

stage of EAE. Besides, Arctigenin treatment reduced the number of silent cells and facilitated normal activity of cells at remission stage.

Arctigenin limits a surge in calcium transient amplitude of cortical neurons at preclinical EAE and reversed calcium influx at remission stage

To characterize the change of intracellular calcium concentration during EAE and Arctigenin treated process, we analyzed the mean amplitude of calcium transient in regions of view. Consistent with previous results, on the 7th day post EAE induction, the calcium transient amplitude increased significantly in vehicle treated EAE mice compared with Arctigenin treated group. Moreover, it's quite unexpected that there were enhancements of calcium transient amplitude in control mice and Arctigenin treated group, while an obvious decrease in vehicle treated mice (Fig. 5a). From the day 6 after induction, the amplitude in vehicle treated EAE group suddenly increased and gradually dropped to the original level, then further decreased to a very low level at late EAE stage. But the increase of calcium transient amplitude in Arctigenin treated mice was slow and moderate in early EAE, like the increase of hyperactive cells described above. What's more, the amplitude of control and Arctigenin treated mice experienced a slight enhancement in late period. This enhancement may be due to chronic and repeated touching mice to operate two-photon imaging (Fig. 5b). In addition, we summarized the amplitude of three groups in preclinical, relapse and remission stage respectively. And we found that the amplitude in vehicle treated mice was significantly increased at preclinical stage, while Arctigenin administration inhibited this preclinical increase (Fig. 5c). However, at the relapse stage, the amplitude began to growing in Arctigenin treated mice and exceeded vehicle treated EAE mice (Fig. 5d). Besides, the amplitude of calcium transient in vehicle treated group significantly decreased at remission stage but Arctigenin reversed this change to some extent (Fig. 5e). Collectively, these results indicate that more calcium influx accompanied with neuronal activity at preclinic EAE stage resulted in functional deficits of cortical cells at remission stage. However, Arctigenin exerted neuronal protection effects through delaying and attenuating the abnormal calcium influx at preclinical stage, indeed decreased silent cells caused by EAE induction.

Restoration of normal functional connectivity and phase synchronization of cortical network by Arctigenin administration at preclinical and remission stage

Functional connectivity is defined as a key indicator of temporal correspondence of calcium transients between two individual neurons. Synchrony is the temporal consistence of distributed neuronal activity, which serves as ability of transferring information among neurons. We used these two parameters to estimate temporal network activity patterns through calculating correlation and synchrony matrices quantifying network functional connectivity (Fig. 6a, left) and synchronization (Fig. 6a, right) among neurons in imaged regions respectively. One week after EAE induction, both of functional connectivity and synchronization of vehicle treated EAE mice were extremely higher in comparison to Arctigenin treated group (Fig. 6a-c). Indeed, at entire preclinical stage, the cortical functional connectivity and synchronization in vehicle treated mice increased starkly and Arctigenin inhibited the abnormal increase (Fig. 6d, f). However, after a long duration of steady enhancement, the functional connectivity continued

to decrease and reached to the lowest level on the day 15 post induction in vehicle treated EAE mice (Fig. 6b). It's worthy to note that from the end of relapse stage, the network connectivity was precipitously elevated and maintained a high level throughout entire remission stage in vehicle treated group (Fig. 6e). Intriguingly, the network synchronization was remained a low level at remission stage in vehicle treated mice, indicating deficits in information transfer (Fig. 6g). But Arctigenin rescued these abnormal effects of EAE induction. In conjunction with the data above, these results suggest the cortical hyperactive microcircuit activity at preclinical stage of EAE, while Arctigenin significantly prevented network hyperactivity and reversed maladaptive functional connectivity and decreased synchrony upon recovery at remission stage.

Arctigenin blunts increased frequency of AMPA receptor-mediated sEPSCs in preclinic EAE

Activation of glutamate AMPA type receptors could trigger calcium influx. Excessively activation of AMPA receptors may result in glutamate excitotoxicity, might contributing to the neuropsychological disorders in MS [28, 29]. We hypothesis that Arctigenin attenuates cortical hyperactivity may act through AMPA receptor mediated synaptic transmission. We recorded AMPA sEPSCs of single neurons in acute cortical brain slices of healthy controls and EAE mice in preclinical stage (day7 to day9 after induction). The frequency of sEPSCs was significantly increased in cells of vehicle-treated EAE mice (0.26 ± 0.03 Hz) in comparison to control mice (0.12 ± 0.01 Hz) and the frequency of sEPSCs was significantly decreased to control level in cells of actigenin-treated EAE mice (0.12 ± 0.01 Hz) (Fig. 7a, c). However, there is no difference in the mean amplitude of sEPSCs between the three groups (Fig. 7b, d). The increased frequency of AMPA receptors mediated sEPSCs, but not amplitude, can be probably explained by a presynaptic enhancement of glutamate transmission, which is compatible with increased neuron activity indicated by Ca^{2+} transients in preclinic stage *in vivo*.

Discussion

In our present study, with chronic real-time two-photon Ca^{2+} imaging in somatosensory cortex, we discovered engagement of cortical hyperactivity at preclinical stage of EAE, including increase in fraction of hyperactive cells, calcium influx into cells, cortical functional connectivity and network synchronization. However, at preclinical stage, mice did not exhibit related clinical symptoms, as measured by the clinical scores. In sharp contrast, EAE mice exhibited a bulk of inactive cells and a few normally active cells at remission stage. Parallel to this, the amplitude of calcium transient in EAE mice was very low in remission stage, which means defective neuronal activity. What's more, the decreased network synchrony at remission stage means poor efficiency of information transmission. As a compensation, the functional connectivity stayed a high level at remission stage to reverse the dysregulation of network circuit in disease progresses [30, 31]. Arctigenin treatment can suppress the hyperactivity phenomenon to a considerable degree at preclinical stage, meanwhile restored neuronal activity and network function at remission stage. Indeed, Arctigenin delayed the onset of clinical symptoms and ameliorated severity. Besides, we did whole-cell voltage clamp patch in acute cortex slices to record the glutamate AMPA receptors sEPSC and found increased frequency of AMPAR sEPSC in

preclinic phase, which can be reversed to normal level by administration of Arctigenin. In conclusion, these results indicate that EAE induction resulted in dysregulated hyperactivity patterns of brain cortex at preclinical stage, including neuronal spiking, calcium influx, network connectivity and synchronization, which was mediated by excessive synaptic transmission. More importantly, Arctigenin can protect cortical neurons by restricting abnormal hyperactivity.

Inflammation response in early period of preclinical stage

In MOG33-35 residues induced EAE model, leukocyte rolling and adhesion is already apparent in the cerebral microvasculature at day 7 after induction [32]. Similarly, the anti-inflammatoty cytokines TGF-β and IL-10 in brain are detectable early in 100ug MOG33-35 induced EAE, with production peaks on the day 7 [33]. The release of IL-17 and IFN-γ on day 7 is observed increased in CNS. TGF-β and IL-6 act concertedly to drive T cell expansion and also differentiation from naïve to a Th17 phenotype [34], or act through activating astrocytes, microglia and antigen presentation in the CNS [35, 36]. Additionally, IL-11 is one of the cytokines which are most highly increased in the cerebrospinal fluid from early RRMS patients, and also can lead to the differentiation and expansion of Th17 cells in MS during the earliest stages [37]. These evidences support that early inflammation has occurred in the CNS of EAE mice at early stage, in which the Th17 cells are the key encephalitogenic population [38]. Importantly, Th17 cells have been reported to form synapse-like contacts with neurons directly, and induce neuronal intracellular Ca^{2+} concentration to undergo serious and localized fluctuation which could be partially reversed, as an early sign of neural damage [39].

Arctigenin restricts cortical hyperactivity in preclinical EAE

Here, we detected more cortical hyperactive neurons in preclinical stage of EAE. Moreover, the calcium transient amplitude was obviously elevated at the same time, which means more calcium influx into cells. Since higher concentration of glutamate increases calcium transient amplitude in excitotoxic situation [40], it's consistent with more proportion of hyperactive neurons we detected in preclinic stage, which facilitates glutamate release and results in more glutamate in cortical extracellular space. Furthermore, the network functional connectivity and synchronization also increased immediately after EAE induction, which indicates dysregulation of cortical microcircuit activity. Of note, we observed the significant increase in fraction of hyperactive neurons from as early as 3rd day after induction. Combining calcium dynamics of single-cell and network circuit, we confirmed the cortical hyperactivity in preclinical stage of EAE, which may be resulted from early inflammation in CNS. Moreover, treatment with Arctigenin exempted EAE mice from cortical severe hyperactivity in preclinical phase, including rapid elevations of neuronal activity and calcium transient amplitude and network connectivity and synchronization. However, recently, Erik Ellwardt et al. applied two-photon Ca^{2+} imaging to assess cortical microcircuits in neuroinflammation in MS. They found the hyperactive cells only in the remission stage not in the preclinical stage [30]. We concluded that the difference between us may be due to the diversity of animal and induction drugs, since proteolipid protein (PLP) and MOG induce different EAE models and autoimmune responses [41]. What's more, they used OGB-1 as calcium indicator which needs to be

loaded to label neurons before imaging in anesthetized mice, while we selected Gcamp6f and repeatedly imaged the same region of cortex in awake mice.

AMPA receptor is involved in excitotoxicity of early EAE

Autoimmune induced glutamatergic upregulation is involved in many disorders, such as Alzheimer [42] and MS [43]. AMPA receptor activation induces calcium influx to participate in pathological pathways, playing an important role in excitotoxicity. In rats with minimal hepatic encephalopathy, peripheral inflammation induces altered hippocampal neurotransmission and impairs spatial learning and memory [44]. It is confirmed that the frequency of AMPA receptor mediated sEPSC is increased at preclinical stage in the striatum of EAE mice with altered GluA1 protein composition of postsynaptic density (PSD) [45]. Moreover, in a previous study, mice with EAE showed increased AMPA receptor expression in hippocampus and sildenafil was able to reduce excitotoxicity by decreasing expression of the receptors [46]. Since activated immune cells release large quantities of glutamate, AMPA/kainite antagonists can reduce autoimmune demyelination and result in substantial amelioration [47]. In our study, we found that there was an evident abnormality of glutamatergic synaptic transmission in cerebral cortex at EAE preclinical stage, considering increased frequency of AMPA receptor sEPSC. This abnormal AMPA receptor mediated transmission may account for the cortical hyperactivity. Furthermore, Arctigenin reversed the frequency of AMPA receptor sEPSC to the normal level, indicating that AMPA receptor mediated neurotoxicity can be compromised by Arctigenin.

Hypoactivity at EAE remission stage can be prevented by Arctigenin

Remission stage is an important and long stage in which patients are allowed to recover from severe clinical symptoms. Notably, we found obviously hypoactivity at EAE remission stage. More neurons became silent and the amplitude of calcium transient reduced to a very low level in vehicle treated EAE mice, reflecting deficits in neuronal activity. Besides, the network synchronization also decreased significantly at remission stage, which means inefficiency information transfer between neurons. Meanwhile, circuit functional connectivity stayed at a maladaptively high level to compromise the hypoactivity, as functional reorganization in brain cortex. However, Arctigenin prevented this hypoactivity phenomenon and restored cortical functional connectivity to normal level at remission stage. Since Multiple lines of evidence support that there is a close correlation between excitotoxicity and neurodegeneration, we guess that at preclinical stage, early inflammatory response cased excessive extracellular glutamate concentration. As a result, AMPA receptors were over activated then facilitated neuronal hyperactivity and abnormal calcium influx. Finally, the massive calcium influx induced excitotoxicity resulted in neuronal activity deficits, poor information transfer and maladaptive functional connectivity at remission stage. However, Arctigenin restricted neuronal hyperactivity and excessive calcium influx at preclinical stage thus protected neurons from excitotoxic injury and death [48, 49] throughout the disease.

Conclusions

In summary, we confirmed the protective effect of Arctigenin on EAE mice mainly in aspects of neuronal activity and network pattern. We have showed that Arctigenin can suppress neuronal hyperactivity and abnormal calcium influx by limiting inordinate glutamate synaptic transmission at EAE preclinical stage, perhaps through attenuating initial immune attack in CNS. Besides, Arctigenin reversed insulted activity of individual neurons and network spike patterns at remission stage. These results suggest that Arctigenin could be a potential therapeutic drug for MS-related neuropsychological disorders at early time.

Abbreviations

MS: Multiple sclerosis

CNS: Central nervous system

EAE: Experimental autoimmune encephalomyelitis

MOG: Myelin oligodendrocyte glycoprotein

AMPA: α-amino-3-hydroxy-5-methyl-4-isoxazolepropionic acid

sEPSC: Spontaneous excitatory postsynaptic current

RS-fMRI: Resting-state functional magnetic resonance imaging

RR: Relapsing-remitting

IL: Interleukin

TNF-α: Tumor necrosis factor-alpha

Bcl-2: B-cell lymphoma-2

Th: T-helper

ACSF: Artificial cerebrospinal fluid

TGF-β: Transforming growth factor-β

IFN-γ: Interferon-gamma

PLP: Proteolipid protein

OGB-1: Oregon Green BAPTA-1

PSD: Postsynaptic density

Declarations

Ethics approval and consent to participate

Animals were purchased from the institute of zoology, Chinese academy of sciences. All experiments were supported by the Animal Care and Use Committee of Tianjin medical university, in accordance with National Institutes of Health guidelines.

Consent for publication

Not applicable.

Availability of data and materials

All data needed to evaluate the conclusions in the paper are present in the paper.

Competing interests

The authors declare no competing interests.

Funding

This work was supported by grants from the National Natural Science Foundation of China (62027812, 81771470) and the Natural Science Foundation of Tianjin, China (19JCQNJC11000).

Authors' contributions

Wei L.P. performed partial two-photon imaging and electrophysiological experiments, wrote the manuscript. Xue Z.Y. performed EAE induction and partial data analysis; Lan B.H. performed partial data analysis; Yuan S.Y. performed partial two-photon imaging; Li Y.Y. performed partial data analysis; Guo C.L. scored clinical symptoms of animals; Zhang R.X. designed the experiments; Ding R. designed the experiments and analyzed partial data; Shen H. designed the experiments and wrote the manuscript. All authors read and approved the final manuscript.

Corresponding author

Correspondence to Rongxin Zhan & Ran Ding & Hui Shen.

Author's information

School of Biomedical Engineering, Tianjin Medical University, 22 Qixiangtai Road, Heping

District, Tianjin, China

Liangpeng Wei, Baihui Lan, Shiyang Yuan, Cunle Guo & Hui Shen

Department of Immunology, Key Laboratory of Immune Microenvironment and Diseases of Educational Ministry of China, Tianjin Key Laboratory of Cellular and Molecular Immunology, Tianjin Medical University, Tianjin, China

Zhenyi Xue

Innovation Institute of Chinese Medicine, Shandong University of Traditional Chinese Medicine, Jinan, China

Yuanyuan Li

Guangdong Province Key Laboratory for Biotechnology Drug Candidates, School of Life Sciences and Biopharmaceutics, Guangdong Pharmaceutical University, Guangzhou, China

Rongxin Zhang

Academy for Advanced Interdisciplinary Studies, Peking University, Beijing, China

Ran Ding

Chinese Institute for Brain Research, Beijing No.26 Science Park Road, ZGC Life Science Park, Changping District, Beijing, China

Ran Ding

Research Institute of Neurology, General Hospital, Tianjin Medical University, Tianjin, China

Hui Shen

References

1. Steinman, L., Immunology of Relapse and Remission in Multiple Sclerosis. Annual Review of Immunology, 2014. 32: p. 257-281.
2. Ontaneda, D., et al., Progressive multiple sclerosis: prospects for disease therapy, repair, and restoration of function. Lancet, 2017. 389(10076): p. 1357-1366.
3. Polman, C.H., et al., Diagnostic criteria for multiple sclerosis: 2005 Revisions to the "McDonald Criteria". Annals of Neurology, 2005. 58(6): p. 840-846.
4. Di Filippo, M., et al., Multiple sclerosis and cognition: synaptic failure and network dysfunction. Nature Reviews Neuroscience, 2018. 19(10): p. 599-609.
5. Fu, J.L., et al., Functional connectivity impairment of postcentral gyrus in relapsin-gremitting multiple sclerosis with somatosensory disorder. European Journal of Radiology, 2019. 118: p. 200-206.
6. Rocca, M.A., et al., Cross-modal plasticity among sensory networks in neuromyelitis optica spectrum disorders. Multiple Sclerosis Journal, 2019. 25(7): p. 968-979.

7. Amato, M.P., et al., Association of MRI metrics and cognitive impairment in radiologically isolated syndromes. Neurology, 2012. 78(5): p. 309-314.
8. Rocca, M.A., et al., Clinical and imaging assessment of cognitive dysfunction in multiple sclerosis. Lancet Neurology, 2015. 14(3): p. 302-317.
9. Acharjee, S., et al., Altered cognitive-emotional behavior in early experimental autoimmune encephalitis–cytokine and hormonal correlates. Brain Behav Immun, 2013. 33: p. 164-72.
10. De Stefano, N., et al., Evidence of early cortical atrophy in MS relevance to white matter changes and disability. Neurology, 2003. 60(7): p. 1157-1162.
11. Peterson, J.W., et al., Transected neurites, apoptotic neurons, and reduced inflammation in cortical multiple sclerosis lesions. Annals of Neurology, 2001. 50(3): p. 389-400.
12. Ben-Nun, A., et al., From classic to spontaneous and humanized models of multiple sclerosis: Impact on understanding pathogenesis and drug development. Journal of Autoimmunity, 2014. 54: p. 33-50.
13. Mahad, D.H., B.D. Trapp, and H. Lassmann, Progressive multiple sclerosis 1 Pathological mechanisms in progressive multiple sclerosis. Lancet Neurology, 2015. 14(2): p. 183-193.
14. Spence, R.D., et al., Bringing CLARITY to gray matter atrophy. Neuroimage, 2014. 101: p. 625-632.
15. Meyer, C.E., et al., Axonal damage in spinal cord is associated with gray matter atrophy in sensorimotor cortex in experimental autoimmune encephalomyelitis. Multiple Sclerosis Journal, 2020. 26(3): p. 294-303.
16. Park, S.Y., et al., Lignans from Arctium lappa and their inhibition of LPS-induced nitric oxide production. Chemical & Pharmaceutical Bulletin, 2007. 55(1): p. 150-152.
17. Gao, Q., M.B. Yang, and Z. Zuo, Overview of the anti-inflammatory effects, pharmacokinetic properties and clinical efficacies of arctigenin and arctiin from Arctium lappa L. Acta Pharmacologica Sinica, 2018. 39(5): p. 787-801.
18. Du, Y.R., et al., Repeated arctigenin treatment produces antidepressant- and anxiolytic-like effects in mice. Brain Research Bulletin, 2019. 146: p. 79-86.
19. Cheng, J.H., et al., Arctigenin ameliorates depression-like behaviors in Toxoplasma gondii-infected intermediate hosts via the TLR4/NF-kappa B and TNFR1/NF-kappa B signaling pathways. International Immunopharmacology, 2020. 82.
20. Zhang, H.B., et al., Synthesis and evaluation of novel arctigenin derivatives as potential anti-Toxoplasma gondii agents. European Journal of Medicinal Chemistry, 2018. 158: p. 414-427.
21. Hyam, S.R., et al., Arctigenin ameliorates inflammation in vitro and in vivo by inhibiting the PI3K/AKT pathway and polarizing M1 macrophages to M2-like macrophages. European Journal of Pharmacology, 2013. 708(1-3): p. 21-29.
22. Jang, Y.P., et al., Arctigenin protects cultured cortical neurons from glutamate-induced neurodegeneration by binding to kainate receptor. Journal of Neuroscience Research, 2002. 68(2): p. 233-240.

23. Zhang, S.M., et al., Arctigenin attenuates ischemic stroke via SIRT1-dependent inhibition of NLRP3 inflammasome. Biochemical and Biophysical Research Communications, 2017. 493(1): p. 821-826.
24. Zhang, N., et al., Neuroprotective effect of arctigenin against neuroinflammation and oxidative stress induced by rotenone. Rsc Advances, 2018. 8(5): p. 2280-2292.
25. Li, W., et al., Arctigenin Suppress Th17 Cells and Ameliorates Experimental Autoimmune Encephalomyelitis Through AMPK and PPAR-gamma/ROR-gammat Signaling. Mol Neurobiol, 2016. 53(8): p. 5356-66.
26. Patel, T.P., et al., Automated quantification of neuronal networks and single-cell calcium dynamics using calcium imaging. Journal of Neuroscience Methods, 2015. 243: p. 26-38.
27. Badura, A., et al., Fast calcium sensor proteins for monitoring neural activity. Neurophotonics, 2014. 1(2): p. 025008.
28. Lau, A. and M. Tymianski, Glutamate receptors, neurotoxicity and neurodegeneration. Pflugers Archiv-European Journal of Physiology, 2010. 460(2): p. 525-542.
29. Potter, L.E., et al., Altered excitatory-inhibitory balance within somatosensory cortex is associated with enhanced plasticity and pain sensitivity in a mouse model of multiple sclerosis. Journal of Neuroinflammation, 2016. 13.
30. Ellwardt, E., et al., Maladaptive cortical hyperactivity upon recovery from experimental autoimmune encephalomyelitis. Nature Neuroscience, 2018. 21(10): p. 1392-+.
31. Di Filippo, M., et al., Synaptic plasticity and experimental autoimmune encephalomyelitis: implications for multiple sclerosis. Brain Res, 2015. 1621: p. 205-13.
32. dos Santos, A.C., et al., CCL2 and CCL5 mediate leukocyte adhesion in experimental autoimmune encephalomyelitis–an intravital microscopy study. J Neuroimmunol, 2005. 162(1-2): p. 122-9.
33. Dias, A.T., et al., Different MOG(35-55) concentrations induce distinguishable inflammation through early regulatory response by IL-10 and TGF-beta in mice CNS despite unchanged clinical course. Cell Immunol, 2015. 293(2): p. 87-94.
34. Veldhoen, M., et al., TGFbeta in the context of an inflammatory cytokine milieu supports de novo differentiation of IL-17-producing T cells. Immunity, 2006. 24(2): p. 179-89.
35. Selmaj, K.W., Tumour necrosis factor and anti-tumour necrosis factor approach to inflammatory demyelinating diseases of the central nervous system. Annals of the Rheumatic Diseases, 2000. 59: p. 94-102.
36. Ferrari, C.C., et al., Reversible Demyelination, Blood-Brain Barrier Breakdown, and Pronounced Neutrophil Recruitment Induced by Chronic IL-1 Expression in the Brain. The American Journal of Pathology, 2004. 165(5): p. 1827-1837.
37. Zhang, X., et al., IL-11 antagonist suppresses Th17 cell-mediated neuroinflammation and demyelination in a mouse model of relapsing-remitting multiple sclerosis. Clinical Immunology, 2018. 197: p. 45-53.

38. Ivanov, II, et al., The orphan nuclear receptor RORgammat directs the differentiation program of proinflammatory IL-17+ T helper cells. Cell, 2006. 126(6): p. 1121-33.
39. Siffrin, V., et al., In Vivo Imaging of Partially Reversible Th17 Cell-Induced Neuronal Dysfunction in the Course of Encephalomyelitis. Immunity, 2010. 33(3): p. 424-436.
40. Schroter, A., et al., Nitric oxide applications prior and simultaneous to potentially excitotoxic NMDA-evoked calcium transients: cell death or survival. Brain Res, 2005. 1060(1-2): p. 1-15.
41. Walczak, A., B. Szymanska, and K. Selmaj, Differential prevention of experimental autoimmune encephalomyelitis with antigen-specific DNA vaccination. Clinical Neurology and Neurosurgery, 2004. 106(3): p. 241-245.
42. Busche, M.A., et al., Clusters of Hyperactive Neurons Near Amyloid Plaques in a Mouse Model of Alzheimer's Disease. Science, 2008. 321(5896): p. 1686-1689.
43. Muhlert, N., et al., Memory in multiple sclerosis is linked to glutamate concentration in grey matter regions. Journal of Neurology Neurosurgery and Psychiatry, 2014. 85(8): p. 834-840.
44. Cabrera-Pastor, A., et al., Peripheral inflammation induces neuroinflammation that alters neurotransmission and cognitive and motor function in hepatic encephalopathy: Underlying mechanisms and therapeutic implications. Acta Physiologica, 2019. 226(2).
45. Centonze, D., et al., Inflammation Triggers Synaptic Alteration and Degeneration in Experimental Autoimmune Encephalomyelitis. Journal of Neuroscience, 2009. 29(11): p. 3442-3452.
46. Araujo, S., et al., Effect of sildenafil on neuroinflammation and synaptic plasticity pathways in experimental autoimmune encephalomyelitis. Int Immunopharmacol, 2020. 85: p. 106581.
47. Pitt, D., P. Werner, and C.S. Raine, Glutamate excitotoxicity in a model of multiple sclerosis. Nature Medicine, 2000. 6(1): p. 67-70.
48. Kornek, B., et al., Distribution of a calcium channel subunit in dystrophic axons in multiple sclerosis and experimental autoimmune encephalomyelitis. Brain, 2001. 124: p. 1114-1124.
49. Ingwersen, J., et al., Nimodipine confers clinical improvement in two models of experimental autoimmune encephalomyelitis. Journal of Neurochemistry, 2018. 146(1): p. 86-98.

Figures

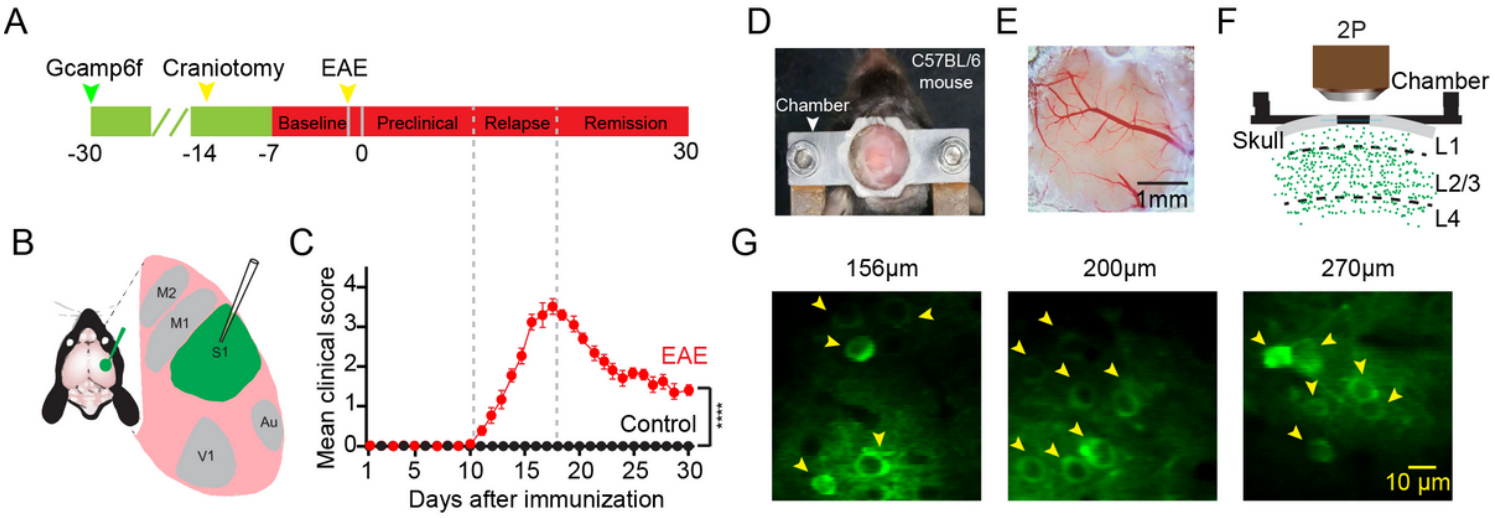

Figure 1

Imaging neuronal activity in somatosensory cortex in awake mice in vivo. a Timeline for two photon imaging of neuronal activity in vivo. Green arrow, indicates virus injection time point; Craniotomy was engaged for chronic imaging; Green line, preparation time for virus expression (about three weeks); Red line represents two-photon imaging time course (about 1 week of pre-imaging for adaption and 1 month after EAE induction). b Illustration of virus injection sites. c Mean daily clinical score of mice recorded from day 1 to day 30 after EAE induction, data shown as mean ± SEM, n=6 mice per group, ****p<0.0001, Two-sample Mann-Whitney test. d Chamber fixed to the cranium of the mouse for chronic two-photon imaging. e Bright field image of a cranial window at somatosensory cortex. f Schematic of two photon imaging process. g Individual in vivo two photon images at different cortical depths in layer 2/3 (left, 156μm; middle, 200μm; right, 270μm).

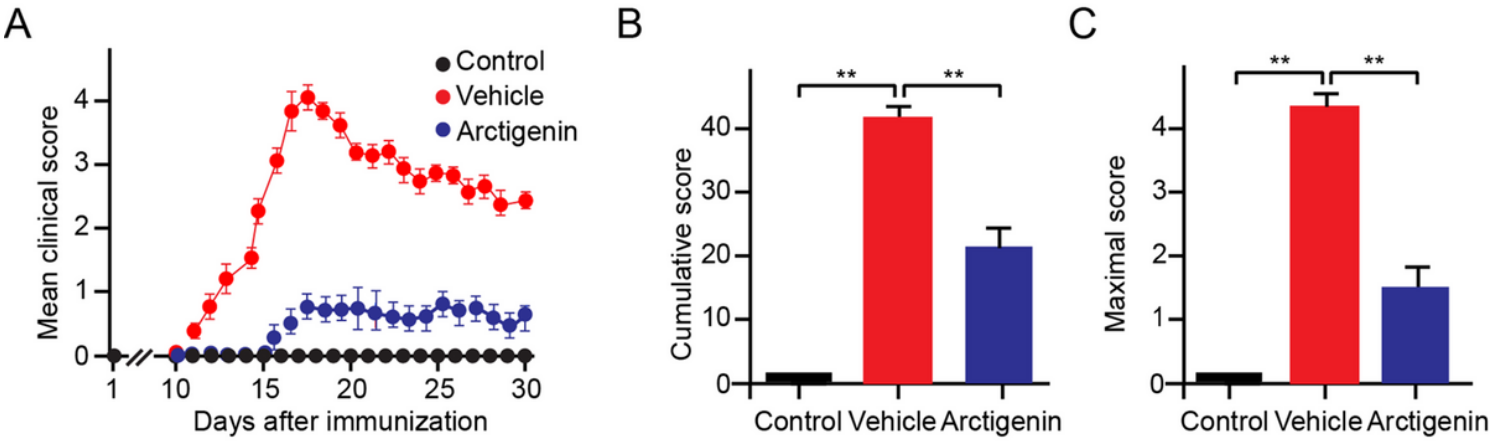

Figure 2

Arctigenin relieves the symptoms of EAE. a Arctigenin was intraperitoneally injected everyday (10 mg/kg) at the beginning after EAE induction. The mean of the daily clinical scores recorded from day 1 to day 30

post-induction after treatment with 10 mg/kg Arctigenin. b The mean of the total of the daily clinical scores observed between day 1 and day 30. c The maximum clinical score of individual mice between day 1 and day 30. All data are expressed as mean ± SEM, n=6 mice per group, **p<0.01, one way ANOVA with Kruskal-Wallis test.

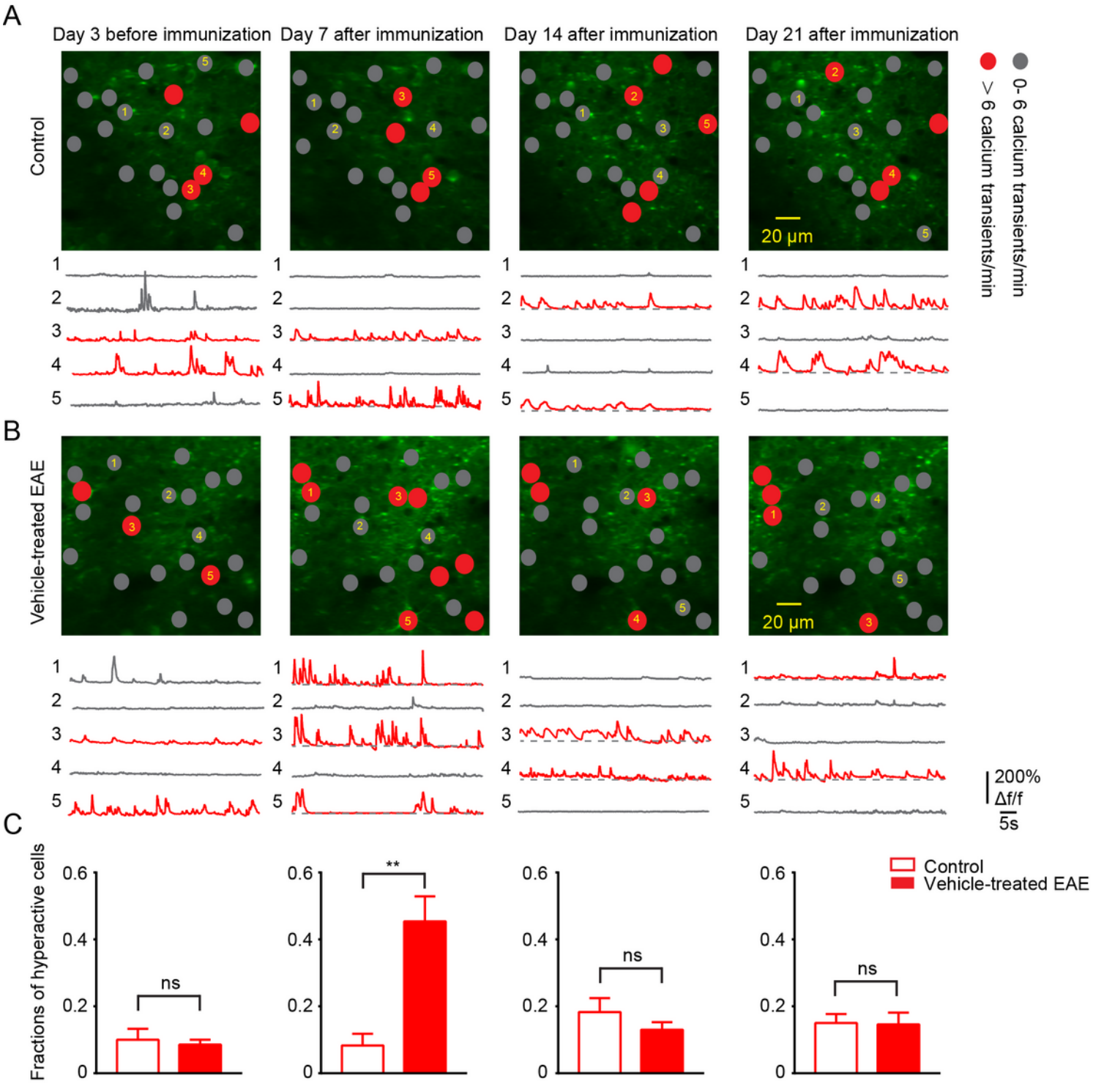

Figure 3

More hyperactive neurons in somatosensory cortex in preclinical stage of EAE. a, b Top, representative images and activity maps in layer 2/3 cortical neurons in 3 days before and 7, 14, 21 days after EAE induction (from left to right) in control a and vehicle-treated EAE mice b. Gray solid circle means 0- 6 Ca2+ transients/min and red solid circle means >6 Ca2+ transients/min (hyperactive cells); Bottom, calcium transients of the marked neurons. c Quantitative data of fraction of hyperactive cells in imaged regions for a, b on the 3 days before induction (n=9 images from 3 mice in control group and n=11 images from 4 mice in vehicle-treated EAE group), the 7th day (n=9 images from 3 mice in control group and n=20 images from 4 mice in vehicle-treated EAE group), the 14th day (n=9 images from 3 mice in control group and n=11 images from 4 mice in vehicle-treated EAE group) and the 21st day (n=9 images from 3 mice in control group and n=10 images from 4 mice in vehicle-treated EAE group) after induction. Data are shown as mean ± SEM., **P < 0.01, ns, not significant, Two-sample Kolmogorov-Smirnov test.

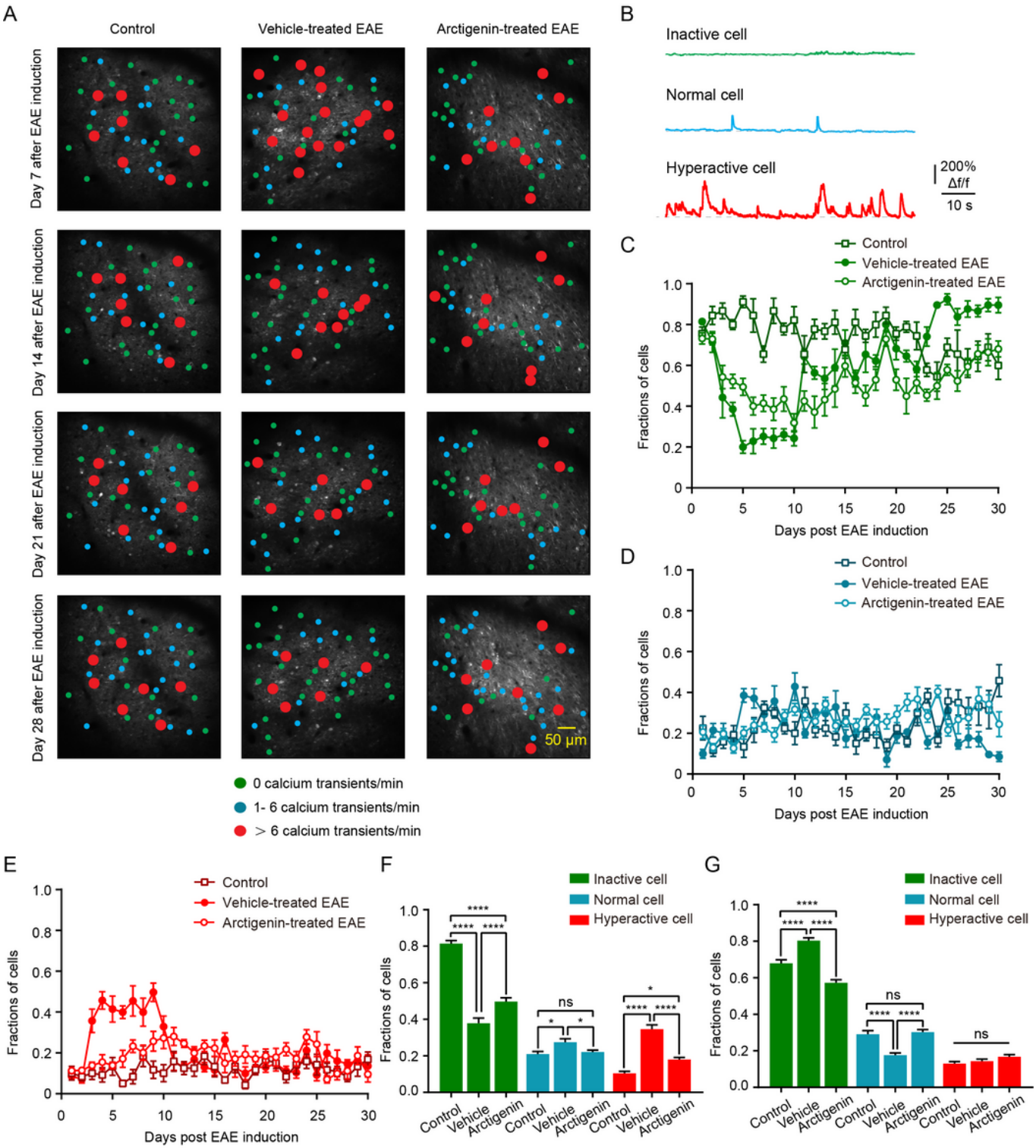

Figure 4

Arctigenin decreased hyperactive neurons at preclinical stage and inactive neurons at remission stage of EAE. a Representative image and activity map in layer 2/3 cortical neurons on day 7, day 14, day 21 and day 28 after EAE induction in control (left), vehicle-treated (middle) and Arctigenin-treated mice (right). b Neurons are categorized into three types based on the frequency of spontaneous calcium transients. Inactive cells are depicted in green (no Ca2+ transient), normal in blue (1- 6 Ca2+ transients/min), and

hyperactive in red (> 6 Ca2+ transients/min). c, d, e Daily fractions of inactive cells c, normal cells d and hyperactive cells e in imaged regions during chronic recording, n=180 images in 3 control mice, n=210 images in 4 vehicle treated EAE mice, n=210 images in 4 Arctigenin treated EAE mice. f Integrated fraction of three category cells in control (n=60 images in 3 mice), vehicle-treated (n=70 images in 4 mice) and Arctigenin-treated (n=70 images in 4 mice) group at preclinic stage, *P < 0.05, ****P < 0.0001, ns, not significant, one way ANOVA with Kruskal-Wallis test. g Integrated fraction of three category cells in control (n=72 images in 3 mice), vehicle-treated (n=84 images in 4 mice) and Arctigenin-treated (n=84 images in 4 mice) group at remission stage, ****P < 0.0001, ns, not significant, one way ANOVA with Kruskal-Wallis test.

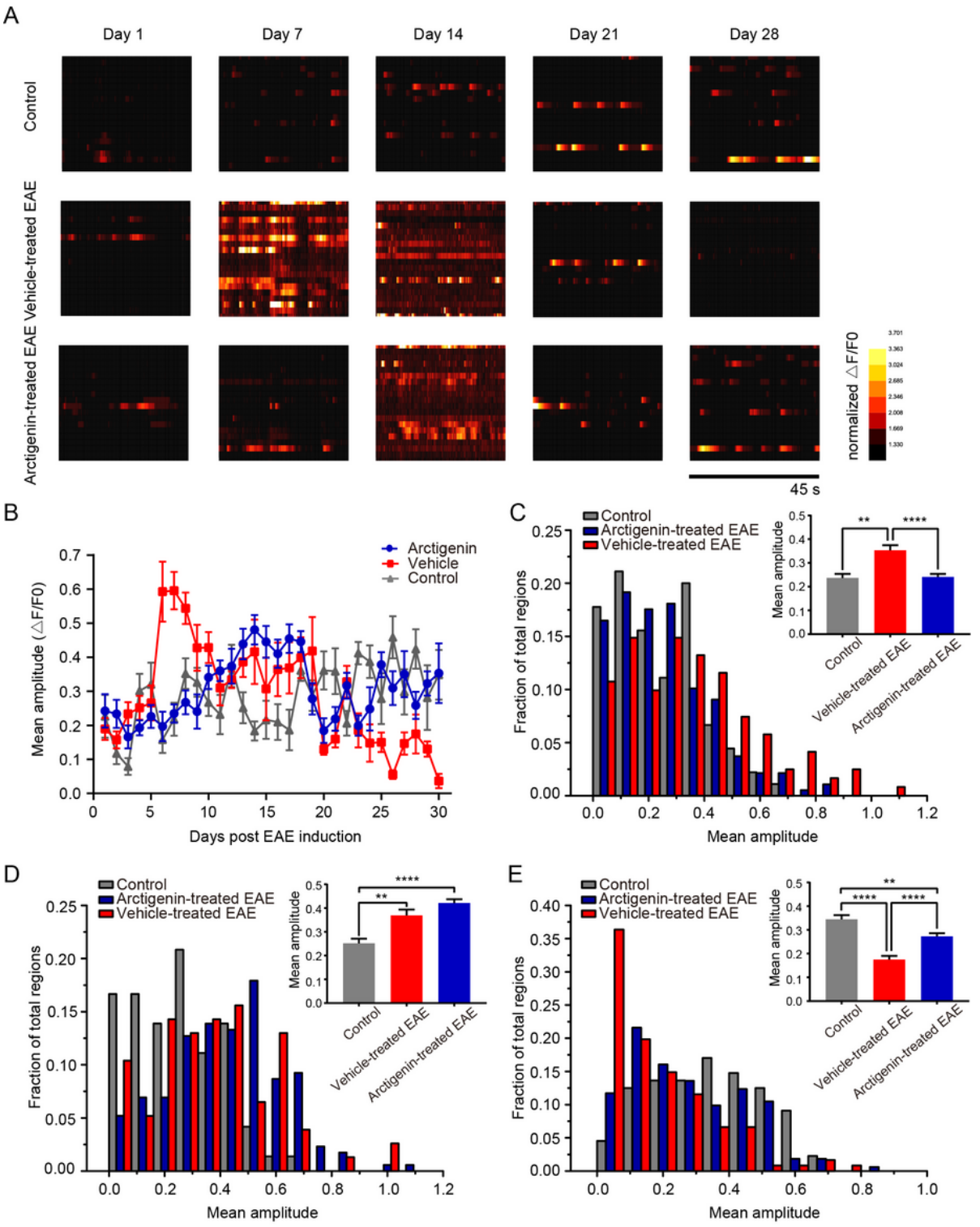

Figure 5

Arctigenin modulated the change of calcium transient amplitude induced by EAE. a Heat maps depicting changes in the calcium transient amplitude (ΔF/F0) for a representative neuronal population at different time point in control mice, vehicle treated EAE mice and Arctigenin treated EAE mice. Each row represents a single cell. The amplitude of each cell is normalized to the minimum value of its own calcium transient. b Mean calcium transient amplitude of imaged regions daily after EAE induction. c, d, e Cumulative

distribution histogram and statistical histogram (inset) of calcium transient amplitudes for integration of three stages respectively, including preclinical stage (c, n=99 images in 3 control mice, n=129 images in 4 vehicle treated EAE mice, n=160 images in 5 Arctigenin treated EAE mice), relapse stage (d, n=72 images in 3 control mice, n=77 images in 4 vehicle treated EAE mice, n=206 images in 5 Arctigenin treated EAE mice) and remission stage (e, n=99 images in 3 control mice, n=126 images in 4 vehicle treated EAE mice, n=245 images in 5 Arctigenin treated EAE mice), **p < 0.01, ****p < 0.0001, one way ANOVA with Kruskal-Wallis test.

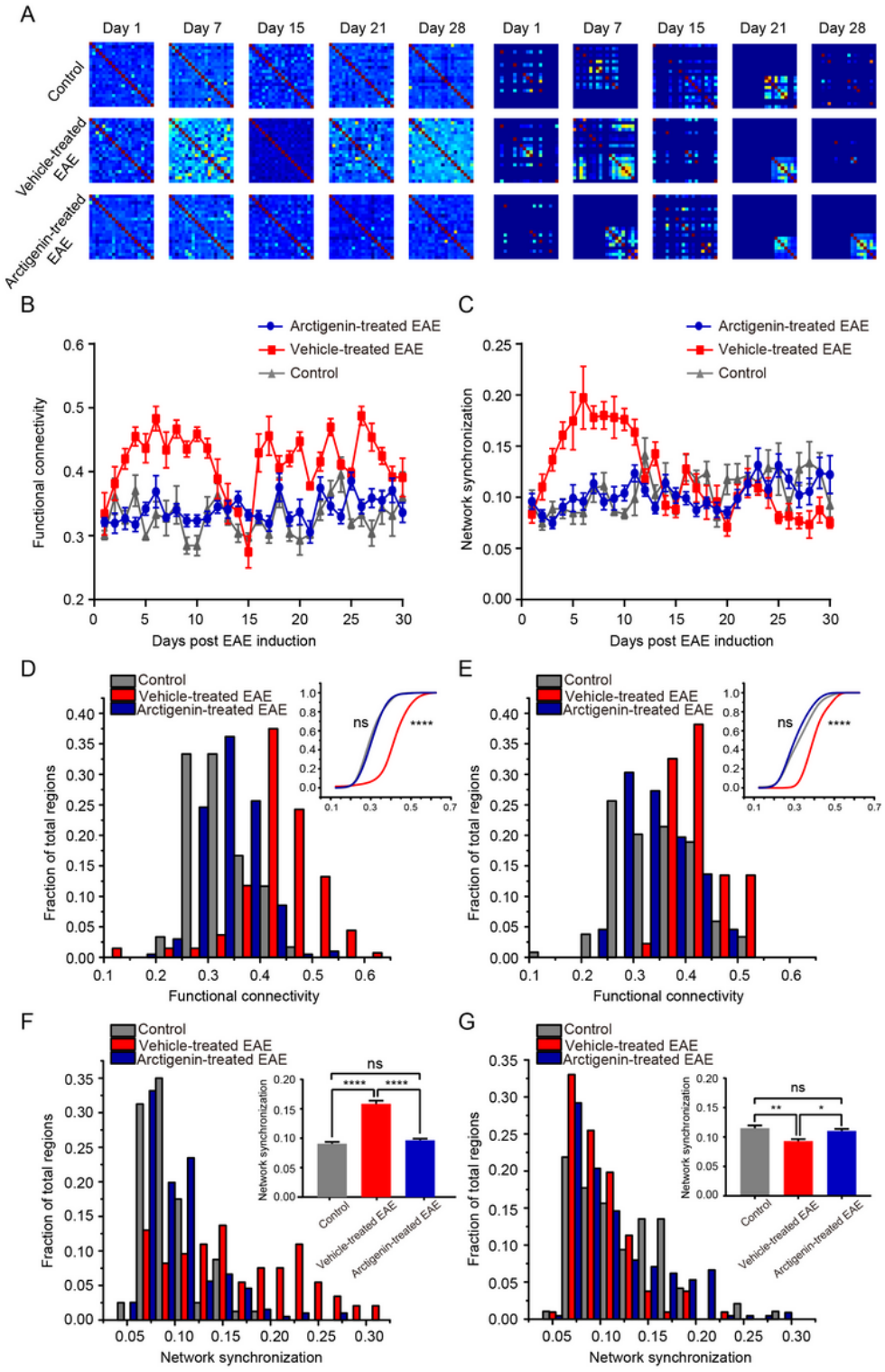

Figure 6

Restoration of functional connectivity and synchronization of cortical network by Arctigenin administration in EAE mice. a Representative correlation matrices measuring network functional connectivity (left) and phase synchronization between each cell and every other cell over time during process of EAE and Arctigenin treatment. b The value of functional connectivity for daily observation. c The value of network synchronization for daily observation. d Distribution histogram and cumulative distribution (inset) of integrated cortical functional connectivity at preclinical stage, n=60 images in 3 control mice, n=129 images in 4 vehicle treated EAE mice, n=187 images in 5 Arctigenin treated EAE mice, control vs Arctigenin treated EAE, ns, not significant; Arctigenin treated EAE vs vehicle treated EAE, ****$p < 0.0001$, one way ANOVA with Kruskal-Wallis test. e Distribution histogram and cumulative distribution of integrated cortical functional connectivity at remission stage, n=66 images in 3 control mice, n=100 images in 4 vehicle treated EAE mice, n=245 images in 5 Arctigenin treated EAE mice, control vs Arctigenin treated EAE, ns, not significant; Arctigenin treated EAE vs vehicle treated EAE, ****$p < 0.0001$, one way ANOVA with Kruskal-Wallis test. f Distribution histogram and statistical histogram (inset) of integrated network synchronization at preclinical stage, n=80 images in 3 control mice, n=146 images in 4 vehicle treated EAE mice, n=196 images in 5 Arctigenin treated EAE mice, ****$p < 0.0001$, ns, not significant, one way ANOVA with Kruskal-Wallis test. g Distribution histogram and statistical histogram of integrated network synchronization at pemission stage, n=96 images in 3 control mice, n=106 images in 4 vehicle treated EAE mice, n=226 images in 5 Arctigenin treated EAE mice, **$p < 0.01$, *$p < 0.05$, ns, not significant, one way ANOVA with Kruskal-Wallis test.

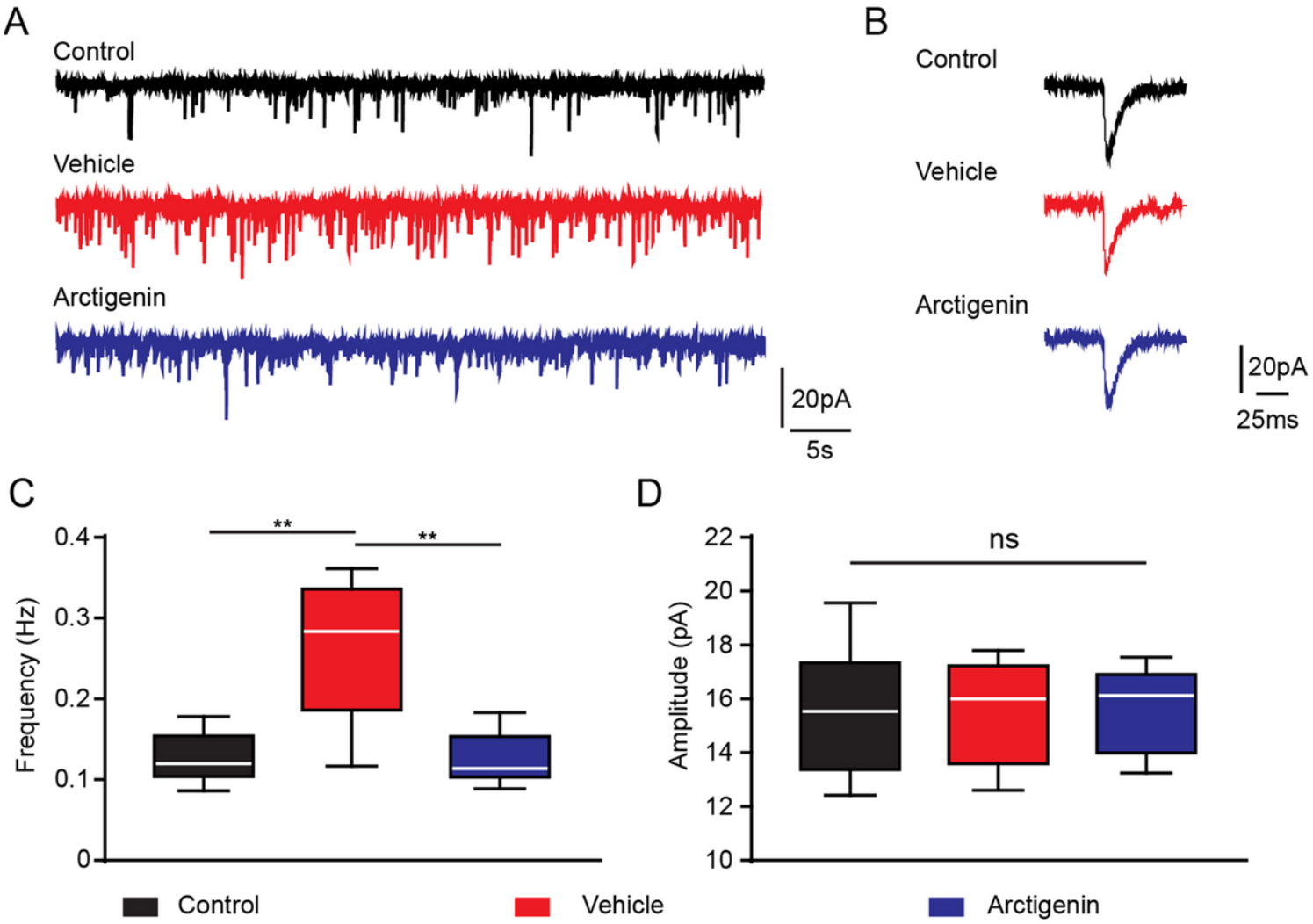

Figure 7

Arctigenin modulates AMPA receptor-mediated sEPSCs. a Representative current traces of pharmacologically isolated AMPA-receptor-mediated sEPSCs in the three groups (black, control group; red, vehicle-treated group; blue, Arctigenin-treated group). b Representative traces of individual sEPSC. c, d Quantification of sEPSC frequency c and amplitude d. Box-and-whisker plot indicates the median value (center line), the 25-75th percentile (box) and the 10-90th percentile (whiskers), n=10 neurons from 4 control mice, n=11 neurons from 5 vehicle-treated mice, n=8 neurons from 4 Arctigenin-treated mice, **P < 0.01, one way ANOVA with Kruskal-Wallis test.